Preprints of the 21st IFAC World Congress (Virtual)
Berlin, Germany, July 12-17, 2020

Clinical application of a model-based cardiac stroke volume estimation method

Rachel Smith * **Joel Balmer** * **Christopher G. Pretty** *
Geoffrey M. Shaw ** **J. Geoffrey Chase** *

* *Department of Mechanical Engineering, University of Canterbury, New Zealand (e-mail: rachel.smith@pg.canterbury.ac.nz).*
** *Christchurch Hospital Intensive Care Unit*

Abstract: A system is needed for monitoring stroke volume (SV) and cardiac output (CO) in unstable patients which is non-additionally invasive, reproducible and reliable in a variety of physiological states. This study evaluates SV estimation accuracy of a non-additionally invasive pulse contour analysis method implemented using a 3-element Windkessel model. The model lumps the properties of the arterial system into 3 parameters: characteristic impedance of the proximal aorta (Z), and resistance (R) and compliance (C) of the systemic arteries. Parameter products ZC and RC are dynamically identified from measured femoral arterial pressure waveforms, and Z is a static parameter obtained by calibration. The accuracy of the model is evaluated for a cohort of 9 liver transplant patients, using thermodilution as a reference method. Data were obtained from Vital Data Bank (VitalDB). The study thus provides independent assessment of a pulse contour analysis, proven in animal studies, in an uncontrolled clinical environment. The model tracked trends in SV well over the course of the surgery. However, the 95% range for percentage error was -88% to +53%, outside acceptable limits of ±45%. Main areas contributing to error for the model include the changing extent of reflected waves in the arterial system, dynamic response characteristics of fluid-filled pressure catheters, and the assumption of fixed Z parameter. Further investigation is needed to consider the contribution of these factors to SV estimation error by the model.

Keywords: Pulse contour analysis, Pressure contour analysis, Windkessel model, Stroke volume, Cardiac output, Hemodynamic monitoring, Intensive care

1. INTRODUCTION

Stroke volume (SV) and cardiac output (CO) are important metrics for hemodynamic management of unstable patients, providing information on blood flow out of the heart beat-by-beat and on average, respectively. SV and CO measured in real-time are useful for evaluating patient status and response to therapy and diagnosing and managing circulatory failure (Cecconi et al. (2014); Reuter et al. (2003); Huygh et al. (2016); Luecke and Pelosi (2005); Busse et al. (2013)). For intensive surgeries, such as liver transplantation, monitoring of SV and CO is necessary and invasive CO monitoring with a pulmonary artery catheter is standard practice (Kashimutt (2017); Rudnick et al. (2015)).

Further work is needed to develop a non-additionally invasive monitoring system for SV or CO, which is reproducible and reliable in a variety of physiological states (Mehta and Arora (2014)). The clinical gold standard monitoring method for CO, pulmonary artery indicator dilution, is invasive and intensive (Grensemann (2018); Busse et al. (2013)). Non-additionally invasive pulse contour analysis methods use only an arterial waveform to estimate CO. However, current clinically available non-additionally invasive devices have insufficient accuracy for monitoring patients during liver transplantation (Rudnick et al. (2015)). The pulse contour analysis model presented by Balmer et al. (2020) does not require any additional patient invasion or new external devices and was able to accurately monitor SV across changing hemodynamic state for pig trials. This study evaluates the SV estimation accuracy of this model for 9 liver transplantation patients.

2. METHODS

2.1 Clinical Data Selection

The data were obtained from Vital Data Bank, a public database of clinical time-series physiological signals (Lee and Jung (2018)). These data are time synchronized recordings from anaesthesia devices made using a data acquisition system called Vital Recorder, collected in accordance with relevant guidelines and regulations of the Institutional Review Board of the Seoul National University Hospital (study H-1408-101-605) and registered at clinicaltrials.gov (NCT02914444).

Patients were selected from the data bank which had the following signals continuously recorded:

- Femoral arterial blood pressure waveform (P_{mea})
- Central venous blood pressure waveform (P_{cvp})
- Electrocardiogram (ECG)
- SV from Vigilance II system (SV_{mea})

Signals were recorded with a sampling frequency of 500 Hz, with the exception of SV, which was recorded at 0.5 Hz.

The Vigilance II system (Edwards Lifescience, Irvine, CA, USA) uses a Swan Ganz catheter and pulmonary artery thermodilution to measure SV and CO. This approach is considered the clinical gold standard (Majumdar (2017)), and provides a calibration and validation SV metric for the model.

Of the patients with the required signal recordings, patients were selected with recordings of more than 5 hours and without ECG abnormalities. The resulting study cohort consisted of 9 liver transplantation patients: 8 male, 1 female; ages ranging from 37 - 71 years; and weights ranging between 59 - 78 kg.

To test the ability of the model to track changes in SV over the course of the liver transplantation surgery, SV was evaluated using the model at half hour intervals over the course of the surgery. At each interval, a 1 minute section (∼100 heartbeats) of physiological signals was used as input to the pulse contour analysis model.

2.2 Signal Processing

P_{mea} was filtered to remove high frequency noise with a low pass Hamming filter with a cut-off frequency and transition width of 7 Hz and 5 Hz, respectively. The filtered P_{mea} signal was used for all subsequent analysis. P_{cvp} did not require filtering as only the average central venous pressures for each beat ($\overline{P}_{cvp}$) are used in this analysis.

2.3 Pulse Contour Analysis Model

The 3-element windkessel model is a lumped parameter model representing the cardiovascular system, shown in Fig 1 (Westerhof et al. (2009, 2010); Frank (1990)). It relates pressure and flow in the large arteries by describing arterial properties using three parameters: characteristic impedance (Z) represents resistance to flow into the windkessel / reservoir; reservoir compliance (C); and resistance (R) to flow leaving the reservoir and and emptying into the venous system (Westerhof et al. (2009, 2010)). The pressure of the downstream venous system is assumed to be constant over a given beat, and equal to the average central venous pressure during that beat, $\overline{P}_{cvp}$.

The model uses an arterial pressure waveform (P_{mea}) as an input, in this case measured at the femoral artery. P_{mea} is divided into a reservoir pressure component (P_{res}) associated with filling of the reservoir, and an excess pressure component (P_{ex}):

$$P_{mea}(t) = P_{ex}(t) + P_{res}(t) \tag{1}$$

P_{ex} represents the pressure drop caused by ejecting blood into the systemic circulation and is thus is directly proportional to flow into the circulation (Q_{in}) for this model:

$$Q_{in}(t) = \frac{P_{ex}(t)}{Z} \tag{2}$$

Assuming this lumped parameter model adequately describes arterial dynamic properties, Q_{in} is equivalent to flow into the aorta (Wang et al. (2003)). Hence, SV (SV_{est}) is estimated by integrating Equation 2 over one beat:

$$SV_{est,\,n} = \frac{1}{Z} \int_{t_{0,n}}^{t_{0,n+1}} P_{ex}(\tau)\, d\tau \tag{3}$$

where the nth beat begins at the P_{mea} waveform foot $t_{0,n}$ and ends at the following waveform foot $t_{0,n+1}$. The pressure waveform foot, which marks the beginning of systole, is detected using a shear transform algorithm similar to in Balmer et al. (2018).

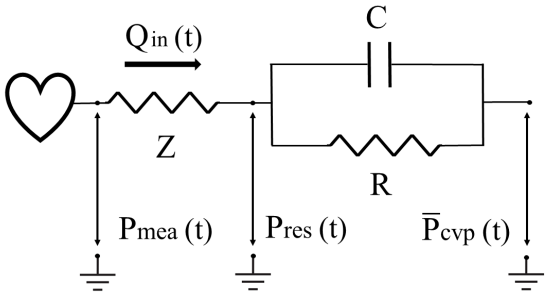

Fig. 1. Schematic representation of the 3-element windkessel model. Q_{in} is flow into the reservoir, P_{mea} is a measured arterial pressure waveform, P_{res} is the modelled reservoir pressure, and $\overline{P}_{cvp}$ is the downstream pressure.

2.4 Model parameter identification

The reservoir pressure waveform (P_{res}) can be calculated from P_{mea} by identifying parameter products RC and ZC. These parameter products can be identified from P_{mea} on a beat-wise basis as an optimization problem by enforcing the condition there is no flow into the aorta during diastole, i.e $P_{ex} = 0$ in diastole (Balmer et al. (2020)). This parameter identification method requires accurate detection of the beginning of diastole / end of systole, found using a weighted second derivative algorithm (Balmer et al. (2020)) identifying end systole as a region of downward concavity in the P_{mea} waveform. End systole detection, identification of RC and ZC, and calculation of P_{res} is described in full by Balmer et al. (2020). Knowing P_{res}, Equation 1 can then be used to calculate P_{ex}.

To calculate beat-to-beat SV from P_{ex} via Equation 3, the remaining model parameter Z must be identified. Z is a lumped parameter modelling the impedance to flow in the large conduit arteries as a resistance. In this study, Z is set to a single constant value, obtained through calibration. The first 1 minute section is used as a control section for calibration of Z against the validation SV metric (SV_{mea}), using a rearrangement of Equation 3:

$$Z_{control,\,n} = \frac{1}{SV_{mea,\,n}} \int_{t_{0,n}}^{t_{0,n+1}} P_{ex}(\tau)\, d\tau \tag{4}$$

$Z_{control,\,n}$ values for all beats of the control section are averaged to reduce the impact of measurement noise, obtaining a single value $\overline{Z}_{control}$, that is then used for calculation of SV_{est} for all time sections.

2.5 Analysis

SV error (ml) and percentage error (%) are calculated using average SV_{est} and SV_{mea} for each 1 minute section. The agreement between SV_{mea} and SV_{est} is assessed using Bland-Altman analysis (Altman and Bland (1983)). In this analysis, the median bias has been used as no assumption is made about how error is distributed.

3. RESULTS

The percentage errors in SV_{est} for each patient are compared to SV_{mea} in the Bland-Altman plot in Fig 2. The distribution of percentage error is shown by the cumulative distribution function (CDF) in Fig 3. Fig 4 shows changes in model input pressures (P_{mea} and P_{cvp}), model output SV (SV_{est}), and validation SV (SV_{mea}) over the duration of the surgery for all patients in the study. Additionally, some examples of P_{mea} and P_{res} waveform shapes are provided in Appendix A, demonstrating variability in pressure waveform shape within and between patients.

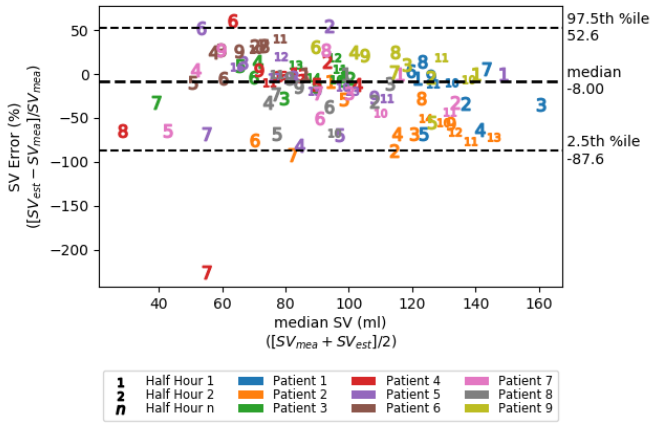

Fig. 2. Bland Altman analysis showing agreement between SV_{mea} and SV_{est} at each time section for each patient.

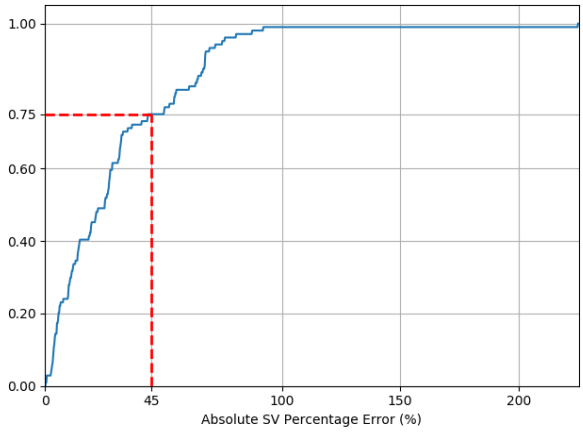

Fig. 3. CDF for absolute percentage error in SV_{est}. The red line indicates proportion of errors falling within 45% error.

4. DISCUSSION

4.1 Hemodynamic response during surgery

Across the duration of the surgeries and 9 patients, a range of arterial pressures and SVs were observed, providing a sufficient test for whether the model can track SV across changing hemodynamic state. Liver transplantation surgery is very complex and leads to numerous hemodynamic challenges, including hemorrhage, low systemic vascular resistance states, and sudden preload change when the liver is reperfused (Kashimutt (2017)). Hence, these data provide a rigorous test for the method. A variety of waveform shapes were observed across and within patients as shown in Figs A.1 - A.3. These differences result from variation in catheter location and arterial properties between patients, and changing patient state over the course of the surgeries.

4.2 Stroke Volume estimation performance

The model generally shows reasonable trending ability to track changes in SV over the course of the surgery, as shown in Fig 4. However, SV_{est} does fluctuate somewhat more than SV_{mea}, following fluctuations in pulse pressure of P_{mea}. The error in SV_{est} does not tend to grow over the course of the surgery, suggesting the model would not require / be improved by re-calibration.

Fig 2 shows percentage errors are large in magnitude with 95% of errors falling within a range of -87% to 52.6%. This range is outside the ±45% criteria reported by Peyton and Chong (2010), using thermodilution as a reference method. Fig 3 shows just over 70% of errors fall within this range.

While the model generally tracked trends well, the agreement of this pulse contour method with thermodilution did not meet suggested criteria. There are a number of limitations contributing to the higher error for these clinical data than for previous validation from pig trials (Balmer et al. (2020)).

4.3 Limitations

Insufficient dynamic response characteristics of fluid filled pressure catheters, used to measure P_{mea}, can alter the pressure waveform shape and render the waveform unsuitable for pulse contour analysis (Grensemann (2018); Gardner (1981)). For example, the Patient 7 pressure waveform shows systolic overshoot at 2.5 and 5 hours (Fig A.3), which occurs for under-damped pressure catheters. This behaviour leads to higher systolic pressures and more area under the P_{ex} waveform, and thus overestimation of SV by the model at these times (Fig 4). Moreover, over- or under- damping is likely to obscure the region in which end systole occurs, leading to inaccurate calculation of the reservoir pressure waveform.

Insufficient dynamic response characteristics of fluid filled pressure catheters is a crucial limitation of using pulse contour analysis models clinically because approximately 30% of arterial waveforms in ICU are either over- or under-damped, and detecting and correcting these requires regular operator intervention (Romagnoli et al. (2014); Gardner (1981)). The effect of this issue could be mitigated

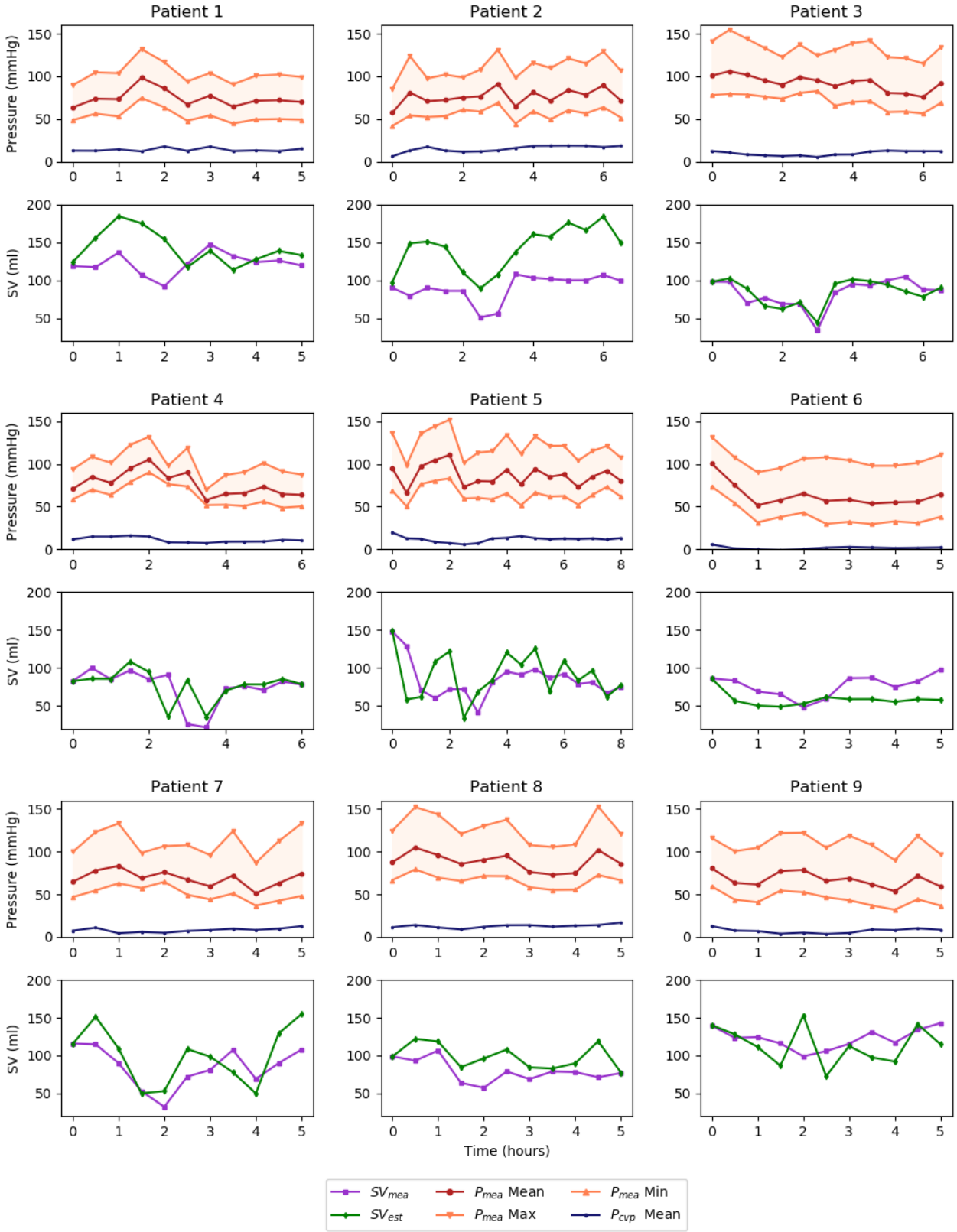

Fig. 4. Femoral arterial mean pressure (P_{mea}), P_{cvp}, modelled SV (SV_{est}), and validation SV (SV_{mea}) over the duration of the liver transplantation surgery for all patients. Pressure mean, maximum, and minimum values are calculated beat-wise, and averaged over each 1 minute time section. SVs are averaged over each 1 minute time section.

by estimating the dynamic response characteristics of the catheter and correcting for them, or avoided altogether by using solid-state pressure catheters, which do not have this limitation.

The 3-element windkessel model does not account for changing wave reflection behaviour of the arterial system. The forward propagating pressure pulse wave is reflected at numerous sites, and these backward reflected waves sum with the forward wave to give the measured pressure signal (Avolio et al. (2009)). Wave reflection can lead to a second pressure peak in diastole, such as in the P_{mea} waveform for Patient 4, at 2.5 hrs (Fig A.3). As the model assumes an exponential decay in diastole, a large reflected wave leads to a poor estimate of reservoir and excess pressure waveform shapes, and inaccurate identification of end systole. While model calibration can account for errors due to wave reflection to some extent, the model will not be robust against changes to the extent of wave reflection caused by changing vascular tone. Future work involves investigating incorporating changing wave reflection behaviour into the pulse contour analysis model.

Pressure changes at the femoral artery may not fully reflect changes at the proximal aorta. However, the femoral artery is a central catheter location, which is commonly used clinically, and predicts aortic pressures more accurately than peripheral sites, such as the radial artery, in liver surgery (Lee et al. (2015)) and patients with septic shock (Kim et al. (2013), Galluccio et al. (2009)). Moreover, peripheral waveforms are distorted more by wave reflection (Westerhof et al. (2010)). Thus, given measuring pressure at the proximal aorta is highly invasive and not clinically feasible, the femoral artery likely represents the best catheter location. A transfer function estimating the aortic pressure waveform from a femoral waveform (Swamy et al. (2009)) would partially address this issue, but accuracy would still be limited by the limited information provided by the input femoral pressure waveform.

In developing a clinically applicable, non additionally invasive method, the result is a simplistic model lumping complex arterial characteristics into only 3 parameters. It is possible model simplicity means it cannot capture all the necessary information required to relate the blood pressure waveform to cardiac output with high accuracy under the changing hemodynamic states. In particular, fixing the Z parameter to a constant value may limit the ability of the model to capture resistance changes associated with conduit arteries. Investigating how the model can be altered to capture changing vascular state, such as low systemic vascular resistance states, represents future work of the author.

5. CONCLUSION

This study uses a pulse contour analysis model that has been previously validated in pigs and applies it to human clinical data acquired from Vital Data Bank. This provides independent validation of a pulse contour analysis model, using measurements from an uncontrolled clinical environment. The model qualitatively captured trends in SV reasonably well, but accuracy fell outside required limits. Several areas were identified that can to contribute to error, including insufficient dynamic response of fluid filled pressure catheters, changing extent of reflected waves in the arterial system, and the assumption of a fixed Z parameter. Investigating the contribution of these factors and how they can be resolved is the future work of the authors.

ACKNOWLEDGEMENTS

This study was supported with funding from the New Zealand Tertiary Education Commission Medtech CoRE, University of Canterbury Doctoral Scholarship, and EU H2020 R&I programme (MSCA-RISE-2019 call) under grant agreement #872488 - DCPM.

REFERENCES

Altman, D.G. and Bland, J.M. (1983). Measurement in Medicine: The Analysis of Method Comparison Studies. *The Statistician*, 32(3), 307.

Avolio, A.P., Van Bortel, L.M., Boutouyrie, P., Cockcroft, J.R., McEniery, C.M., Protogerou, A.D., Roman, M.J., Safar, M.E., Segers, P., and Smulyan, H. (2009). Role of pulse pressure amplification in arterial hypertension: experts' opinion and review of the data. *Hypertension*, 54(2), 375–83.

Balmer, J., Pretty, C., Davidson, S., Desaive, T., Kamoi, S., Pironet, A., Morimont, P., Janssen, N., Lambermont, B., Shaw, G.M., and Chase, J.G. (2018). Pre-ejection period, the reason why the electrocardiogram Q-wave is an unreliable indicator of pulse wave initialization. *Physiological Measurement*, 39(9), 095005.

Balmer, J., Pretty, C.G., Davidson, S., Mehta-Wilson, T., Desaive, T., Smith, R., Shaw, G.M., and Chase, J.G. (2020). Clinically applicable model-based method, for physiologically accurate flow waveform and stroke volume estimation. *Computer Methods and Programs in Biomedicine*, 185, 105125.

Busse, L., Davison, D.L., Junker, C., and Chawla, L.S. (2013). Hemodynamic monitoring in the critical care environment. *Advances in chronic kidney disease*, 20(1), 21–29.

Cecconi, M., De Backer, D., Antonelli, M., Beale, R., Bakker, J., Hofer, C., Jaeschke, R., Mebazaa, A., Pinsky, M.R., Louis, J., Jean, T., Vincent, L., Rhodes, A., Cecconi, M., Rhodes, Á.A., De Backer, D., Vincent, J.L., Antonelli, M., Beale, R., Bakker, J., Hofer, C., Jaeschke, R., Diderot, P., Sorbonne, P., Cité, P., Aphp, L., Pinsky, M.R., and Teboul, J.L. (2014). Consensus on circulatory shock and hemodynamic monitoring. Task force of the European Society of Intensive Care Medicine. *Intensive Care Med*, 40(12), 1795–1815.

Frank, O. (1990). The basic shape of the arterial pulse. First treatise: Mathematical analysis. *Journal of Molecular and Cellular Cardiology*, 22(3), 255–277.

Galluccio, S.T., Chapman, M.J., and Finnis, M.E. (2009). Femoral-radial arterial pressure gradients in critically ill patients. *Critical care and resuscitation*, 11(1), 34–8.

Gardner, R.M. (1981). Direct blood pressure measurement-dynamic response requirements. *Anaesthesiology*, 54(3), 227–236.

Grensemann, J. (2018). Cardiac Output Monitoring by Pulse Contour Analysis, the Technical Basics of Less-Invasive Techniques. *Frontiers in Medicine*, 5, 64.

Huygh, J., Peeters, Y., Bernards, J., and Malbrain, M. (2016). Hemodynamic monitoring in the critically ill: an overview of current cardiac output monitoring methods [version 1; peer review: 3 approved]. *F1000Research*, 5(2855).

Kashimutt, S. (2017). Anaesthesia for liver transplantation. *BJA Education*, 17(1), 35–40.

Kim, W.Y., Jun, J.H., Huh, J.W., Hong, S.B., Lim, C.M., and Koh, Y. (2013). Radial to Femoral Arterial Blood Pressure Differences in Septic Shock Patients Receiving High-Dose Norepinephrine Therapy. *Shock*, 40(6), 527–531.

Lee, H.C. and Jung, C.W. (2018). Vital Recorder—a free research tool for automatic recording of high-resolution time-synchronised physiological data from multiple anaesthesia devices. *Scientific Reports*, 8(1), 1527.

Lee, M., Weinberg, L., Pearce, B., Scurrah, N., Story, D.A., Pillai, P., McCall, P.R., McNicol, L.P., and Peyton, P.J. (2015). Agreement between radial and femoral arterial blood pressure measurements during orthotopic liver transplantation. *Critical care and resuscitation*, 17(2), 101–107.

Luecke, T. and Pelosi, P. (2005). Clinical review: Positive end-expiratory pressure and cardiac output. *Critical care (London, England)*, 9(6), 607–621.

Majumdar, M. (2017). Haemodynamic Monitoring in the Intensive Care Unit. In *Intensive Care*. InTechOpen.

Mehta, Y. and Arora, D. (2014). Newer methods of cardiac output monitoring. *World journal of cardiology*, 6(9), 1022–1029.

Peyton, P.J. and Chong, S.W. (2010). Minimally Invasive Measurement of Cardiac Output during Surgery and Critical Care. *Anesthesiology*, 113(5), 1220–1235.

Reuter, D.A., Kirchner, A., Felbinger, T.W., Weis, F.C., Kilger, E., Lamm, P., and Goetz, A.E. (2003). Usefulness of left ventricular stroke volume variation to assess fluid responsiveness in patients with reduced cardiac function. *Critical Care Medicine*, 31(5), 1399–1404.

Romagnoli, S., Ricci, Z., Quattrone, D., Tofani, L., Tujjar, O., Villa, G., Romano, S.M., and De Gaudio, A.R. (2014). Accuracy of invasive arterial pressure monitoring in cardiovascular patients: an observational study. *Crit. Care*, 18(6), 644.

Rudnick, M.R., de Marchi, L., and Plotkin, J.S. (2015). Hemodynamic monitoring during liver transplantation: A state of the art review. *World Journal of Hepatology*, 7(10), 1302–1311.

Swamy, G., Xu, D., Olivier, N.B., and Mukkamala, R. (2009). An adaptive transfer function for deriving the aortic pressure waveform from a peripheral artery pressure waveform. *American Journal of Physiology*, 297(5), H1956–63.

Wang, J.J., O'Brien, A.B., Shrive, N.G., Parker, K.H., and Tyberg, J.V. (2003). Time-domain representation of ventricular-arterial coupling as a windkessel and wave system. *American Journal of Physiology-Heart and Circulatory Physiology*, 284(4), H1358–H1368.

Westerhof, N., Lankhaar, J.W., and Westerhof, B.E. (2009). The arterial Windkessel. *Medical & Biological Engineering & Computing*, 47(2), 131–141.

Westerhof, N., Stergiopulos, N., and Noble, M.I.M. (2010). *Snapshots of Hemodynamics*. Springer, New York.

Appendix A. ADDITIONAL RESULTS

This appendix contains examples of P_{mea} and P_{res} waveforms for several patients, demonstrating the variation in waveform shapes within and between patients.

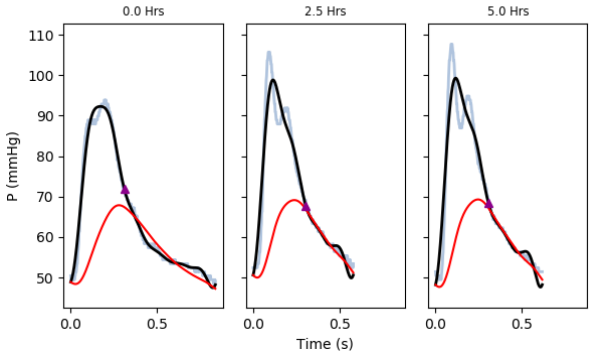

Fig. A.1. Example of P_{mea} and P_{res} waveform for a single beat at several time points through the surgery for Patient 1

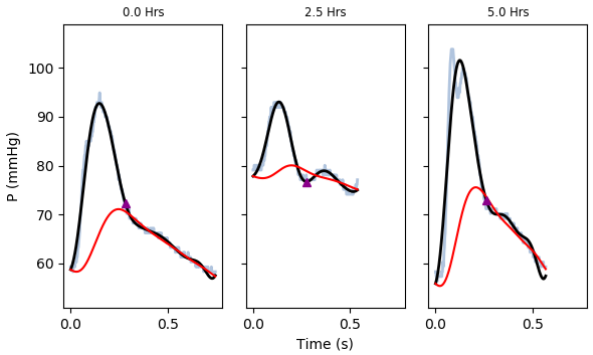

Fig. A.2. Example of P_{mea} and P_{res} waveform for a single beat at several time points through the surgery for Patient 4

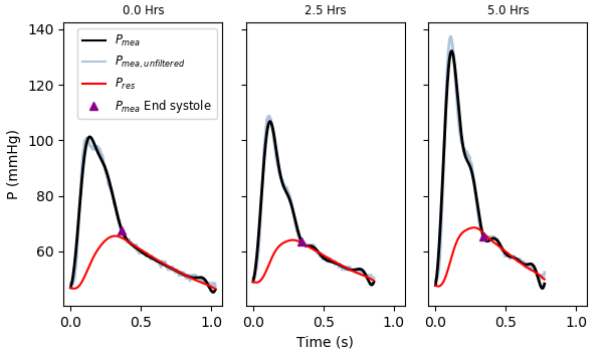

Fig. A.3. Example of P_{mea} and P_{res} waveform for a single beat at several time points through the surgery for Patient 7